Electroencephalogram-Driven Machine-Learning Scenario for Assessing Impulse Control Disorder Comorbidity in Parkinson's Disease Using a Low-Cost, Custom LEGO-Like Headset

Wei-Che Lin, Wei-Jen Chen, Yueh-Sheng Chen, Hsing-Yi Liang, Cheng-Hsien Lu, and Yuan-Pin Lin, *Member, IEEE*

***Abstract*— Patients with Parkinson's disease (PD) may develop cognitive symptoms of impulse control disorders (ICDs) when chronically treated with dopamine agonist (DA) therapy for motor deficits. Motor and cognitive comorbidities critically increase the disability and mortality of the affected patients. This study proposes an electroencephalogram (EEG)-driven machine-learning scenario to automatically assess ICD comorbidity in PD. We employed a classic Go/NoGo task to appraise the capacity of cognitive and motoric inhibition with a low-cost, custom LEGO-like headset to record task-relevant EEG activity. Further, we optimized a support vector machine (SVM) and support vector regression (SVR) pipeline to learn discriminative EEG spectral signatures for the detection of ICD comorbidity and the estimation of ICD severity, respectively. With a dataset of 21 subjects with typical PD, 9 subjects with PD and ICD comorbidity (ICD), and 25 healthy controls (HC), the study results showed that the SVM pipeline differentiated subjects with ICD from subjects with PD with an accuracy of 66.3% and returned an around-chance accuracy of 53.3% for the classification of PD versus HC subjects without the comorbidity concern. Furthermore, the SVR pipeline yielded significantly higher severity scores for the ICD group than for the PD group and resembled the ICD vs. PD distinction according to the clinical questionnaire scores, which was barely replicated by random guessing. Without a commercial, high-precision EEG product, our demonstration may facilitate deploying a wearable computer-aided diagnosis system to assess the risk of DA-triggered cognitive comorbidity in patients with PD in their daily environment.**

***Index Terms*— Computer-aided diagnosis, electroencephalogram, impulse control disorder, low-cost headset, machine learning, Parkinson's disease.**

I. Introduction

PARKINSON'S disease (PD) is a common neurodegenerative disease that manifests as disabling symptoms of motor function, such as tremors, rigidity, postural instability, and gait disturbance [3]. Patients with PD may experience comorbidities of impulse control disorders (ICDs) when treated with dopamine agonist (DA) therapy for motor deficits [5], [6], [7]. ICDs refer to cognitive and motor impulsivity and lead to entangling dysfunctions in the control of reward-based decision and motor response inhibition [5], [8], [9], which may facilitate compulsive gambling, sexual behavior, buying, and eating [6]. These emergent disorders significantly affect the quality of life of the affected patients and their families and caregivers [7]. The main approach to preventing such DA side effects involves either decreasing the DA dose or switching to another dopamine replacement therapy, but this undermines the agonist-treated motor benefits [7] and causes worsening motor dysfunction [11]. Accordingly, a better understanding of ICD mechanisms and their objective assessments will benefit the development of preventive and therapeutic strategies to ameliorate adverse effects of DA during chronic pharmacotherapy for PD motor symptoms [6], [7], [8], [12].

Human brain imaging and mapping techniques that analyze brain signals with or without task engagement of interest, such as functional magnetic resonance imaging (fMRI) [7], [12] and electroencephalography (EEG) [5], [8], [13], may shed light on qualitatively and quantitatively probing the underlying neural mechanisms of active ICDs in patients with PD. Despite the unique merits of different imaging modalities in terms of spatial and temporal details, their reports share common

Manuscript received 6 June 2023; revised 10 September 2023; accepted 9 October 2023. Date of publication 11 October 2023; date of current version 24 October 2023. This work was supported in part by the Collaborative Research Project of National Sun Yat-sen University and Kaohsiung Chang Gung Memorial Hospital, Taiwan, under Grant 109-08; and in part by the Higher Education Sprout Project of National Sun Yat-sen University, Ministry of Education, Taiwan. *(Corresponding author: Yuan-Pin Lin.)*

This work involved human subjects or animals in its research. Approval of all ethical and experimental procedures and protocols was granted by the Institutional Review Board of Chang Gung Medical Foundation.

Wei-Che Lin and Yueh-Sheng Chen are with the Department of Diagnostic Radiology, Kaohsiung Chang Gung Memorial Hospital, and the College of Medicine, Chang Gung University, Kaohsiung 83301, Taiwan (e-mail: alex@cgmh.org.tw; yssamchen@gmail.com).

Wei-Jen Chen and Hsing-Yi Liang were with the Institute of Medical Science and Technology, National Sun Yat-sen University, Kaohsiung 804201, Taiwan (e-mail: welkins1211@gmail.com; liangyi1104@gmail.com).

Cheng-Hsien Lu is with the Department of Neurology, Kaohsiung Chang Gung Memorial Hospital, and the College of Medicine, Chang Gung University, Kaohsiung 83301, Taiwan (e-mail: chlu99@cgmh.org.tw).

Yuan-Pin Lin is with the Institute of Medical Science and Technology and the Department of Electrical Engineering, National Sun Yat-sen University, Kaohsiung 804201, Taiwan (e-mail: yplin@mail.nsysu.edu.tw).

Digital Object Identifier 10.1109/TNSRE.2023.3323902

evidence that alternation or abnormality of brain activation in the frontal lobe is associated with impairment of inhibitory control (i.e., cognitive and motor impulsivity) in patients with PD and ICD symptoms compared with patients with typical PD. Pioneering fundamental studies corroborate the potential of characterizing brain activity markers, offering the capability to assess individuals with PD who are at risk of developing ICDs during dopaminergic mediation.

The EEG modality is a cost-efficient and user-friendly recording scenario for measuring electrical brain activity with excellent temporal resolution. Its wearability facilitates the customization of an EEG-sensing module by leveraging either onboard or remote signal processing and decoding to preferable EEG markers for different objectives, such as a standalone brain–computer interface (BCI) control solution for neuromotor deficits [15], a brain-actuated exoskeleton for poststroke rehabilitation [17], and a head-mounted display-incorporated EEG device to objectively assess visual deficits in glaucoma [19]. Moreover, an EEG scenario boosts the leap in clinical assessment from the hospital to the daily environment, which is challenging with other imaging modalities (e.g., fMRI). Previous successful demonstrations of realistic application-deployable EEG-sensing infrastructure motivate the development of software and hardware modules tailored to capture ICD-related EEG signatures and diagnose cognitive comorbidities in patients with PD.

Machine-learning methods are commonly used to learn a set of discriminative EEG markers and subsequently shape a predictive model for the automatic diagnosis of motor and cognitive symptoms in patients with PD. Predictive decision-making aims to provide a complementary assessment to the traditional diagnostic approaches of subjective evaluation or questionnaire scales for PD. It is particularly important because early non-motor symptoms are mild and often overlooked in clinical practice [2]. Table I lists representative EEG studies that have focused on PD assessment using machine learning. The majority of studies have tackled the discrimination of patients with PD from healthy controls using resting EEG data and reported high classification accuracies (81−99%) [1], [2], [4], [10], [14], [16] through different methodological frameworks (e.g., feature extraction, classification, and validation procedures). Follow-up attempts have been devoted to resolving specific PD stages and progressions (e.g., early vs. late PD [18]) or motor defects (e.g., freezing of gait (FOG) vs. normal walking [20]). Moreover, cognitive impairment is frequently observed in patients with PD and coincides with motor dysfunctions [23]. Motor and non-motor comorbidities critically increase disability and mortality in affected patients. The machine-learning scenario is also applicable to exploiting predictive EEG markers and classifiers to characterize non-motor symptoms and facilitate early diagnosis [21], [22], [23]. Cognitive assessment scenarios have been reported with an accuracy of 66–88%, including identifying PD with mild cognitive impairment (MCI) [21], categorizing the severity of cognitive impairments into five phenotypes from intact to severely deficient [22], and predicting future cognitive worsening [23]. Taken together, the machine-learning framework incorporating EEG signature processing (e.g., extracting temporal or spectral signatures as features) enables the learning of targeted EEG markers and constructs a predictive model for the assessment of motor and non-motor disabling symptoms or subtypes of PD. This facilitates the development of a computer-aided diagnosis (CAD) system for objective screening, prognostic monitoring, and early detection in clinical practice. Nevertheless, the generalizability of the CAD pipeline for PD must be thoroughly demonstrated. Given a limited dataset, cross validation (CV) is commonly adopted by splitting the data into training and test folds to optimize and report the performance of a predictive model. Because data samples from the same individuals inherently resemble each other, a subject-wise CV method should be considered to prevent suspicious links between the training and test data to realistically verify the generalizability of the proposed machine-learning model against unseen/unlearned data from a new subject [24].

Inspired by encouraging ICD-relevant EEG endeavors [5], [8], [13] and remarkable success in machine-learning-assisted diagnosis in PD (particularly for cognitive impairments) [21], [22], [23], this study attempted to construct an EEG-driven machine-learning scenario to identify ICD symptoms in patients with PD and further predict ICD severity (i.e., an ICD-aware CAD system) in compliance with a generalizable subject-wise CV procedure. Unlike most of the previous machine learning-based studies focusing on different aspects of PD (e.g., diagnose, staging, MCI comorbidity), this study is the first one, to the best of our knowledge, that assesses DA-associated ICD comorbidities in patients with PD using a machine-learning scenario. Notably, instead of using commercial high-precision EEG-sensing products, this study customized a low-cost, compact EEG-sensing hardware assembly to record EEG signals, which is considered an emerging challenge for user-friendly BCI hardware [25]. From both the therapeutic and prognostic perspectives, the successful demonstration greatly promotes the deployment of wearable BCI-based CAD infrastructure to routinely monitor ICDs of patients with PD as per the targeted EEG markers in their living environments to prevent ICD worsening or recurrence during chronic pharmacological treatments for motor symptoms.

II. Methods

This study is a follow-up to a previous study [13] that preliminarily assessed temporal event-related potential (ERP) signatures of ICD severity in patients with PD using a simple univariate linear regression analysis. We followed the same experimental protocol and data-collection setup to obtain data from a few more subjects and then demonstrated the applicability of a multivariate machine-learning approach to assess PD and ICD comorbidities. The following subsections describe the developed low-cost wearable EEG instrument, cognitive task used to appraise ICD responses, and data analysis framework. They also clarify the applicability of the proposed EEG hardware and software infrastructures to deployable BCI-based cognitive assessments.

A. Low-Cost LEGO-Like Electrode Headset and Instrument

Developing a user-friendly, compact, and wearable EEG-sensing device is considered a major challenge in facilitating the transition from laboratory demonstrations

TABLE I
REPRESENTATIVE EEG STUDIES FOCUSING ON MACHINE-LEARNING SCENARIOS IN PD

Work	Task	Methods (feature + classifier)	Validation	Accuracy
Yuvaraj *et al.* [1] 2016	Resting	Spectral features + SVM	Sample-wise 10-fold CV	PD vs. HC: 99.62%
Oh *et al.* [2] 2018	Resting	Temporal features + CNN	Sample-wise 10-fold CV	PD vs. HC: 88.25%
Lee *et al.* [4] 2021	Resting	Spectral features + CRNN	Sample-wise 10-fold CV	PD vs. HC: 99.2%
Chu *et al.* [10] 2021	Resting	Spectral features + CNN	Sample-wise 8-fold CV	PD vs. HC: 99.87%
Chang *et al.* [14] 2022	Resting	Spectral features + Bagging	Subject-wise 10-fold CV	PD vs. HC: 81%
Khoshnevis *et al.* [16] 2022	Resting	HOS features+ Bagged DT	Subject-wise LSO CV	PD vs. HC: 99.19%
Khoshnevis *et al.* [18] 2021	Resting	HOS features + RUSBoosted tree	Subject-wise LSO CV	Early PD vs. late PD: 86.4%
Handojoseno *et al.* [20] 2015	Walking	Spectral features + MLP	Sample-wise CV	FOG vs. NW: 80.2%
Zhang *et al.* [21] 2021	Resting	Spectral features + SVM	Subject-wise validation	PD-MCI vs. PD-NC: 66%
Betrouni *et al.* [22] 2019	Resting	Spectral features + KNN	Subject-wise validation	Cognitive profiles: 88%
Arnaldi *et al.* [23] 2017	Resting	Spectral features + LDA	LOO CV*	Cognitive worsening: 82%

*CNN: convolutional neural network; CRNN: convolutional neural network + recurrent neural network; CV: cross validation; DT: decision tree; ELM: extreme learning machine; FOG: freezing of gait; HC: healthy control; HOS: higher order statistics, LOO: leave-one-out; LR: logistic regression; LSO: leave-one-subject-out; MLP: multilayer perceptron neural network; MCI: mild cognitive impairment; NC: normal condition; NW: normal walking; PD: Parkinson's disease; SVM: support vector machine; *: the manner to evaluate follow-up sessions of an individual is not fully disclosed.*

to practical applications in real-life settings [25]. Instead of employing expensive commercial medical-grade EEG recording products with high precision in signal quality, this study used a cost-efficient, laboratory-developed EEG instrument consisting of an arm-attached eight-channel amplifier [26] and a LEGO-like electrode-holder assembly infrastructure [27] (Fig. 1A). The amplifier measures the EEG signals with a sampling rate of 250 Hz and in a bandwidth of 0.6−56.5 Hz and transmits the digitized signals wirelessly via a Bluetooth protocol. The LEGO assembly offers the unique capability of unlimitedly (re)assembling an electrode montage with respect to the number of electrodes and their positions with a preferred electrode type (e.g., wet, dry, or semi-dry materials; Fig. 1B). A user can intuitively adjust it to ensure better electrode–scalp contact and signal quality iteratively by swapping suitable primary components, for example, an inter-ring bridge with a different length, in accordance with the user's head size and circumference, if necessary. In contrast, most existing commercial EEG headsets have a fixed design by default and are challenging to self-adjust to electrode density and coverage, headset frame size, and electrode types. The efficacy of the amplifier and LEGO headset was empirically verified by capturing classic BCI signatures (e.g., ERP and steady-state visual evoked potential) in the still [13], [26], [27], [28] and walking [29] settings. More details for the design and implementation of the amplifier and LEGO headset can be found in [26] and [27], respectively.

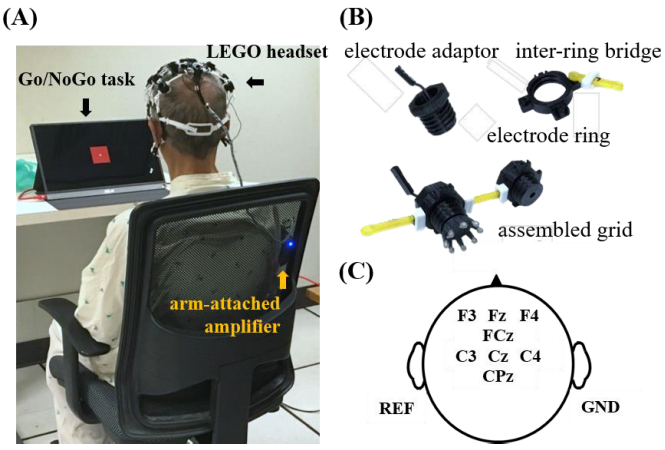

Fig. 1. Cost-efficient, customized EEG instrument used to record EEG signals while performing a visual Go/NoGo task. (A) Recording setup. (B) LEGO-like electrode-holder assembly. (C) 8-ch electrode montage.

In this regard, this study customized an eight-channel LEGO headset wired to the arm-attached amplifier. It accommodated the electrodes at the F3, Fz, F4, FCz, C3, Cz, C4, and CPz locations in the frontocentral area with the left and right earlobes as the reference and ground sites, respectively (Fig. 1C). The frontocentral placement considered the desired cognitive task, namely the Go/NoGo protocol, to be attended to by the participants (described in Section II-B). Dry flexible electrodes (Cognionics, Inc., San Diego, CA, USA) were embedded for

EEG measurements. The LEGO-assembled components can be fabricated using a low-end fused deposition modeling 3D printer [27]. The eight-electrode LEGO headset grid costs approximately 10 USD for filament consumption and assembly accessories (excluding dry electrodes). Considering an amplifier unit (∼150 USD) and its paired event-broadcaster module (∼50 USD) [26], the cost of the EEG collection setup was approximately 210 USD. Such a cost-efficient, customizable, and wearable EEG-sensing hardware infrastructure promotes the future embodiment of routine assessment for each individual with PD in a daily environment.

B. Cognitive Task and Data Collection

To appraise ICD, neuroimaging studies are advised to address task-based and event-related analysis [9]. As mentioned in previous EEG studies, the classic Go/NoGo cognitive task is the prevailing protocol to induce behavioral and neural responses to cognitive and motor inhibition [30], [31] and its validity has been verified in PD with ICD [5], [8], [13]. Thus, this study implemented a Go/NoGo task to record and analyze ICD-related EEG abnormalities. Taking a simple two-target embodiment, the Go/NoGo protocol presents a rapid series of stimulus events (e.g., visual and auditory) with different occurrences: one is a Go target frequently presented, and the other is a rare NoGo target. The deviant NoGo target initiates inhibition control processing (i.e., withholding the prepotent response) from its accompanying Go target, which forces a prompt behavioral response. Successful NoGo reactions ideally result in frontocentral N2 (i.e., a negative deflection in amplitude of approximately 200–300 ms) and P3 (i.e., a positive peak around 300–500 ms) signatures in the ERP profile [30], [31], [32]. This also explains the practicability of the LEGO-like electrode grid, which can be assembled to cover the task-relevant frontocentral region exclusively.

This study implemented a visual Go/NoGo task with target occurrences of 70% and 30% for the Go and NoGo events, respectively. A participant was instructed to press the button as quickly as possible once a green square cue (8.5 cm × 8.5 cm) is presented on a 16" monitor but withhold the button-pressing for a red square cue (Fig. 1A). A single session was composed by three 80-trial blocks (with an inter-trial jitter of 0.5–1.5 s) and resulted in a total of 168 Go trials and 72 NoGo trials. Each participant underwent two Go/NoGo sessions with an approximately one-hour inter-session rest. Each session lasted approximately 30 minutes, in an attempt to allow the older subjects to engage in the task attentively.

The dataset in [13] included 59 subjects divided into three groups: 26 healthy controls (HC group), 23 patients with typical PD (PD group), and 10 patients with PD and ICD comorbidities (ICD group). This study followed the same procedure to recruit more participants from the HC and PD groups (HC: 2; PD: 1). All patients were interviewed by neurologists, diagnosed with idiopathic PD according to the United Kingdom Brain Bank criteria [33], and screened for ICD comorbidity as per the Questionnaire for Impulsive-Compulsive Disorders in Parkinson's Disease Rating Scale (QUIP-RS) [34]. QUIP-RS is a valid and reliable rating scale for monitoring ICD severity over time. Before data collection, each subject completed the QUIP-RS again for data analysis. Clinical assessment and data collection were performed at the Kaohsiung Chang Gung Memorial Hospital (CGMH) in Taiwan. Both the PD and ICD groups underwent the 1st Go/NoGo session at least 12 hours after the last dopaminergic medication intake (i.e., off-state) and were administered their personal medication immediately after completing it (i.e., on-state). As such, this allowed us to capture EEG changes related to the DA-triggered motoric and cognitive inhibition impairments in the 2nd session. Seven subjects (HC: 3, PD: 3, ICD: 1) discontinued the 2nd session due to personal issues or severe artifacts during recording and were excluded (Section II-C). Finally, this study included 55 subjects, including 25 HC (12 men, 13 women; age: 58.6 ± 7.0 years), 21 PD (14 men, 7 women; age: 65.6 ± 8.9 years), and 9 ICD (7 men, 2 women; age: 63.2 ± 7.7 years) subjects for the sequential analysis. The self-reported QUIP-RS score was significantly higher in the ICD group than in the PD group (ICD group: 16.0 ± 12.3; PD group: 0.5 ± 1.1, $p < 0.001$ assessed by a permutation test, see Section II-D for details); thus, using a machine-learning scenario to assess ICD comorbidity in patients with PD was valid.

C. EEG Preprocessing and Feature Extraction

This study followed the preprocessing procedures adopted in [13] to prepare artifact-suppressed EEG trials corresponding to Go and NoGo events per session. The procedure band-pass filtered raw signals into 1−30 Hz, partitioned the filtered signals into trials (−200 to 1000 ms) with baseline correction (-200 to 0 ms), z-score standardized the trials, rejected the noisy trials using a statistical kurtosis threshold (> 4 standard deviations), and discarded mistakenly responded trials. Subjects with less than 80% of completed EEG trials were discarded. The retained 55 subjects had 90.1 ± 5.6% valid trials on average per session (Go: 151.3 ± 11.2 trials; NoGo: 64.9.3 ± 4.6 trials). Subsequently, an extended infomax independent component analysis (ICA) [35] was separately applied to each session to mitigate eye movement artifacts during the visual task. The open-source EEGLab toolbox/scripts [36] were used to perform the preprocessing and ICA procedures described above.

Motivated by previous machine-learning demonstrations in PD (Table I), this study captured EEG spectral contents at time intervals of N2 (200–400 ms) and P3 (400–600 ms) components that were found to differ in the Go versus NoGo contrast in [13]. The spectral power in four frequency bands, including delta (1–3 Hz), theta (4–7 Hz), alpha (8–13 Hz), and beta (14–30 Hz), was calculated to encapsulate spectral changes and their links to patients with PD with or without ICD comorbidity while engaging in the visual Go/NoGo task. Time–frequency (TF) analysis was adopted to characterize the time-evolving spectral perturbations for each trial using the Morlet wavelet transform. Each Go and NoGo event then formed an ensemble of TF outcomes from each session. Its ensemble average can be referred to as the event-related spectral perturbation (ERSP) [37], which depicts the spectral disparity over time after event onset. Based on the session-wise Go and NoGo ensembles, two statistical measures, the peak amplitude and mean amplitude, were used to summarize the band-specific spectral content associated with the preferable time intervals for the N2 and P3 signatures. The between-session contrasts in peak and mean amplitudes (i.e., 2nd – 1st difference) were also derived. This study assumed

that patients with PD and ICD comorbidities exhibit inhibitory control-related EEG spectral signatures disparate from those of patients with typical PD, which is beneficial for ICD assessment using machine learning. In short, the aforementioned spectral feature extraction constituted a 768-dimentional feature space (8 channels × 4 bands × 2 ERP component time spans × 2 statistical measures × 2 events (Go and NoGo) × 3 session settings (1^{st}, 2^{nd}, and 2^{nd}–1^{st} contrast) for sequential machine-learning modeling.

D. Machine Learning and Validation

This study attempted to demonstrate the applicability of a machine-learning framework to identify ICD comorbidity and estimate its severity from Go/NoGo task-engaged EEG oscillations recorded using a low-cost, lab-customized wearable instrument instead of medical-/research-grade high-precision commercial products. We implemented a widely used supervised support vector machine (SVM) algorithm and further adapted it to learn EEG associations with self-reported QUIP-RS scores (i.e., the higher the score, the more severe the ICD) in patients with PD. This issue is addressed by an SVM regressor called the support vector regression (SVR) model. SVM and SVR share the same principle of exploiting a set of hyperplanes (i.e., decision boundaries) to recognize the given labels of the data in the preferable feature space. This can be achieved by incorporating a kernel to project the input data into a higher dimensional space for hyperplane optimization. Once a learning phase is completed, an SVM model enables to classify an unseen data to one of the predefined classes, whereas an SVR model outputs numeric values to the data.

This study constructed two machine-learning scenarios to address ICD comorbidities in patients with PD: 1) SVM modeling for binary classification tasks (i.e., PD vs. HC and ICD vs. PD) and 2) SVR modeling for ICD severity estimation (i.e., PD and ICD). Both the SVM and SVR models were implemented using LIBSVM software [38]. Regarding the SVM tasks, the PD–HC performance was intended to refer to most machine-learning-based PD studies that typically distinguish patients with PD from healthy controls [1], [2], [4], [10], [14], [16] (Table I), whereas the ICD–PD counterpart was used to demonstrate the potential of recognizing patients with PD and ICD comorbidities using machine learning, which has rarely been reported previously. Both the SVM and SVR outcomes further prove the applicability of estimating ICD severity using EEG signatures captured by a low-cost customized EEG-sensing module.

The following procedures were employed to validate the SVM and SVR pipelines. First, leave-subject-out (LSO) validation was used to derive the classification and regression performance while considering model generalizability [24]. That is, the LSO recruited N-1 subjects (N: subject size) as training samples to build and optimize the model and test its performance against the remaining subject as test sample who was never seen/learned during model training. The LSO performance was then derived by averaging N repetitions in which each subject was tested equally. Second, the sample size for the paired subject groups could be highly imbalanced (e.g., HC/PD vs. ICD). Each LSO repetition further replicated the model evaluation 10 times, given randomly selected group-balanced samples, which obviated a plausible prediction bias due to a group with larger training samples. Third, a model optimization procedure was implemented using group-balanced training samples to select the most discriminative features and effective model kernel parameters. Performing feature reduction over the initial 768-dimentioanl feature space by removing redundant or meaningless features effectively dispelled the concern of overfitting owing to the overwhelming feature dimensions against the sample size in this study. The optimized model was subsequently evaluated using a completely disjointed test subject. The other pipeline-specific procedures for feature selection, model kernel, and performance evaluation are as follows.

1) SVM Modeling for Binary Classification: The binary classification task employed a feature selection method, namely, maximum relevance and minimum redundancy (mRMR) [39]. mRMR enables us to iteratively select a subset of features with the highest dependence on the target class (max relevance) and also with the lowest correlation among themselves (min redundancy). In other words, the most discriminative features can be effectively kept given a high dimensional feature space while trimming the redundant ones for machine-learning modeling at lower computational complexity. An optimal and minimal subset of the most discriminative features was retained only for training an SVM classifier with a linear function in each LSO repetition. This study used the metrics of sensitivity, specificity, accuracy, and balanced accuracy (BA) to quantify the efficacy of the trained classifier in differentiating PD subjects from HC subjects (PD vs. HC) or ICD subjects from PD subjects (ICD vs. PD). In particular, the BA quantity is the average of the sensitivity and specificity, which prevents the misinterpretation of a predictive model tailored to a certain group of subjects compared with traditional accuracy.

2) SVR Modeling for ICD Severity Estimation: This study implemented a polynomial kernel-based SVR model to learn the relationships between ICD severity and EEG features for PD subjects (the PD and ICD groups only). ICD severity was defined according to the QUIP-RS score in the range of 0–64. The mean square error (MSE) was used to quantify the performance of the trained SVR model by calculating the average squared difference between the estimated and actual scores. Additionally, an optimal subset of discriminative EEG features associated with a lower MSE was identified to optimize the SVR model. In addition, unlike chance accuracy, which can be used to benchmark the performance of a classification task, we alternatively replicated the aforementioned SVR framework by feeding randomly shuffled EEG-score pairs to the recruited PD subjects during the model training and optimization phases. This randomization was conducted 100 times to obtain an average MSE, which was considered a benchmark for random estimation of ICD severity (named $\text{SVR}_{\text{Random}}$ hereafter).

Finally, a permutation test (implemented in Matlab) was applied to assess the statistical differences in ICD scores between behavioral QUIP-RS, SVR-predicted, and $\text{SVR}_{\text{Random}}$-predicted outcomes for within-group and between-group comparisons. This test shuffled the scores between the groups, resulting in a statistical measure. It then formed a permutation distribution after 10,000 repetitions. The statistical value was then calculated by comparing the actual test statistics with the permutation distribution under the null

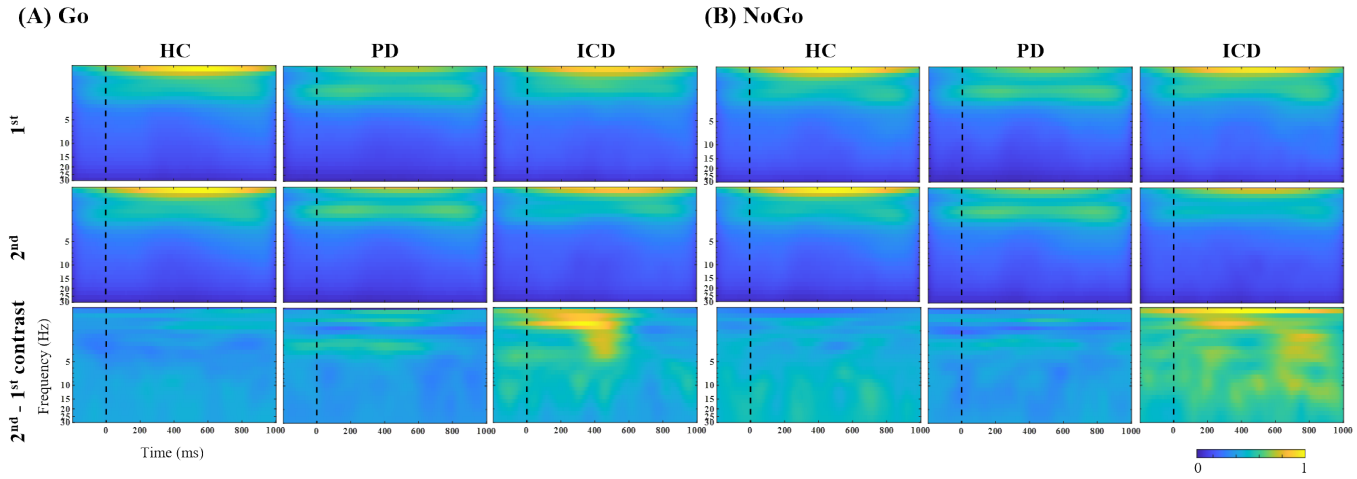

Fig. 2. Session-wise Go and NoGo ERSP and their contrast for each subject group. The participants in the PD and ICD groups had their personal DA treatment after the 1st session.

TABLE II
SVM CLASSIFICATION PERFORMANCE (%)

Metrics	PD vs. HC	ICD vs. PD
Sensitivity	54.3	61.1
Specificity	52.4	68.6
Accuracy	53.3	66.3
Balanced accuracy	53.3	64.8

HC: healthy control; PD: Parkinson's disease; ICD: PD with ICD comorbidity.

hypothesis, which was valid for handling statistical assessments with a small subject size in this study.

III. RESULTS

Fig. 2 illustrates the Go and NoGo ERSP per session and their comparison for each subject group. The single-session results and between-session contrasts were normalized to a range of 0–1 for comprehensive comparison. The three subject groups exhibited dominant spectral changes at low frequencies, (e.g., delta) for single sessions, yet with distinct amplitudes for different groups. While both the PD and ICD groups were treated with their personal DA medication after the 1st session, only the ICD group had considerable spectral disparity distributed across frequencies over time, as shown in the 2nd –1st session contrast, indicating the tendency of ICD-associated EEG disparity when performing the same Go/NoGo task. Most importantly, the resultant spectral contrast in the ICD group manifested at distinct frequencies over certain time intervals, for example, delta and theta activities approximately at 200–500 ms for the Go event and relatively broadband modulations at 200–500 ms and 600–900 ms for the NoGo event. The above qualitative ERSP comparison explained the applicability of encompassing tempo-spectral EEG oscillations as features to estimate ICD comorbidity in patients with PD using machine learning.

Table II lists the performance of the binary classification tasks (i.e., PD vs. HC and ICD vs. PD) using the SVM. The ICD versus PD task returned a higher classification performance than the PD versus HC task for all metrics. In particular, its sensitivity was inferior to the corresponding specificity by 7%; that is, correctly recognizing ICD subjects was relatively challenging compared with recognizing PD subjects. This explains the marginal drop in balanced accuracy from accuracy. Nevertheless, the same SVM modeling pipeline was ineffective in differentiating the EEG signatures of the PD subjects from those of the HC subjects, leading to metric values near the chance level of 50%.

Fig. 3 presents the SVR-predicted ICD scores in the PD and ICD groups with respect to the behavioral QUIP-RS and SVR_{Random} settings. There are several findings worth mentioning as per the within-group (Fig. 3) and between-group (Table III) comparisons in the methodological settings. First, as shown in Fig. 3A, the established SVR model (color-filled) tended to underestimate the actual ICD scores (QUIP-RS, unfilled) in the ICD group; however, this was not statistically significant ($p = 0.13$). In contrast, SVR typically overestimated the ICD scores ($p < 0.01$) in the PD group. Next, random estimation by the SVR_{Random} model (gray-filled) was unlikely to replicate the actual SVR estimation in the ICD group but returned scores far below the QUIP-RS counterpart (both $p < 0.01$). The SVR_{Random} model in the PD group behaved similarly to the actual SVR model ($p = 0.77$) and was associated with overestimated ICD scores ($p < 0.01$). However, as indicated by the between-group comparison in Table III, the ICD group had higher SVR-estimated ICD scores than the PD group ($p = 0.003$), which meaningfully resembled the tendency of the ICD–PD contrast in the QUIP-RS scores ($p < 0.001$). The randomly estimated ICD scores were comparable between the groups ($p = 0.574$).

Finally, despite the SVR-predicted ICD scores (3.86 ± 2.32) in the PD group being considerably lower on average than the actual ICD scores (16.00 ± 12.32, $p < 0.001$) in the ICD group, a few PD individuals (e.g., subjects 12 and 15) could be mistakenly treated as having ICD comorbidity considering the SVR estimation outcome (Fig. 3B). In addition, some ICD individuals (e.g., subjects 1, 3, 7, and 8) with severe ICD comorbidities (i.e., a higher QUIP-RS score) were overlooked. Accordingly, even though misdiagnosis may occur in some individuals, the aforementioned group analysis remained valid

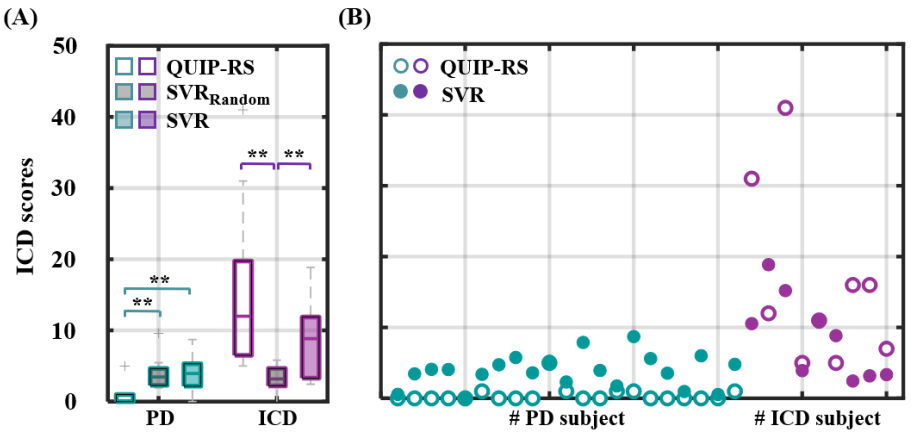

Fig. 3. (A) Group-level and (B) individual-level ICD scores of the PD and ICD groups using behavioral, SVR$_{Random}$, and SVR settings. ** indicates the statistical difference ($p < 0.01$) for the within-group comparison.

TABLE III
ICD SCORES (MEAN AND STANDARD DEVIATION) OF THE PD AND ICD GROUPS USING BEHAVIORAL, SVR $_{RANDOM}$, AND SVR SETTINGS

ICD scores	PD	ICD	p-value$^{\#}$
QUIP-RS	0.48 ± 1.12	16.00 ± 12.32	< 0.001
SVR$_{Random}$	3.67 ± 1.80	3.25 ± 1.77	0.574
SVR	3.86 ± 2.32	8.57 ± 5.86	0.003

HC: healthy control; PD: Parkinson's disease; ICD: PD with ICD comorbidity; QUIP-RS: Questionnaire for Impulsive-Compulsive Disorders in Parkinson's Disease Rating Scale; SVR: support vector regression. $^{\#}$ indicates between-group statistical assessment.

to demonstrate that the proposed SVR pipeline is applicable for estimating ICD severity to some extent in PD using EEG signals.

IV. DISCUSSION

This study empirically demonstrated the applicability of a machine-learning scenario for assessing ICD comorbidities in patients with PD using spectral disparity while engaging attentively in a simple cognitive Go/NoGo task. Such a conceived EEG-based scenario consisting of task engagement, data measurement, and automatic estimation potentially provides an objective neurological assessment along with traditional diagnostic approaches, such as subjective interviews and questionnaires (e.g., QUIP-RS) in clinical practice. To the best of our knowledge, this is the first study to address DA-associated ICD comorbidity in PD, which complements previous machine-learning-assisted endeavors focusing on PD identification, PD staging, or other cognitive aspects of PD [1], [2], [4], [10], [14], [16], [18], [20], [21], [22], [23]. Notably, the EEG measurements in this study were performed using a low-cost, custom EEG headset (a LEGO-like headset) instead of a commercial high-precision medical product. Our demonstration bridges the gap in how to deploy a user-friendly wearable BCI-based CAD device for each individual with PD in a daily environment to routinely monitor ICD risk during pharmacological treatment. The following subsections discuss the validity of the machine-learning outcomes and shape potential future efforts.

A. EEG Spectral Disparity of PD and ICD Comorbidities

Patients with PD and cognitive dysfunction have been reported to exhibit increased low-frequency power in the delta and theta bands and decreased high-frequency power in the alpha and beta bands compared to cognitively typical patients [40]. Spectral changes tended to spread across the scalp instead of focal regions. The middle frontal gyrus-based functional connectivity in the theta band and its altered connectivity patterns have been found to act as reliable markers to identify cognitive impairment [41]. These fundamental findings may explain the rationale of existing machine-learning studies [21], [22], [23] that commonly exploit spectral dynamics as features for estimating cognitive deficits in patients with PD using EEG signals (Table I). For example, a classification model benefited more from the theta activity in the left sensorimotor cortex to distinguish patients with PD that had MCI [21]. Increased delta and theta power can contribute to assessing the severity of cognitive impairment [22]. By contrast, the implemented Go/NoGo task effectively induces an inhibitory process and manifests as frontocentral N2 and P3 alteration [30], [31], [32]. Its applicability has been demonstrated in exploring EEG markers in patients with PD with and without ICDs [5], [8], [13]. While attending to the Go/NoGo protocol, ICDs were associated with decreased beta activity in the precuneus and in the medial frontal cortex over the supplementary motor area (SMA) [5], reflecting the dysfunction of proactive inhibitory control. Even during task-free rest, SMA beta changes have been found to reflect ICD severity [8]. Taken together, PD and ICD comorbidities lead not only to cognitive dysfunction facilitating choice impulsivity but also to motor dysfunctions for action impulsivity [8].

Standing upon aforementioned endeavors in spectral correlates of cognitive capability in patients with PD, this study was motivated to leverage the spectral EEG contents of the frontocentral N2 and P3 signatures to assess ICD comorbidity and its severity. As per the between-group ERSP profiles (Fig. 2), after DA treatment, the ICD group exhibited distinct spectral patterns along with preferable N2 and P3 time spans compared with the PD group, for example delta and theta activities for the Go event and broadband modulations for the NoGo event. By contrast, the PD group without ICD comorbidity was similar the HC group. Thus, a high-dimensional feature space of 768 spectral attributes constituted by N2 and P3 signatures at different frequency bands (i.e., delta, theta, alpha,

and beta) over eight frontocentral electrodes was constructed in this study to boost the capacity to capture ICD-related spectral disparity and sequentially actuate a machine-learning pipeline.

B. Validity of Machine-Learning Findings

In this study, an EEG-based machine-learning scenario was created to detect patients with PD and ICD comorbidity and to estimate the ICD severity. Because no reports have addressed this issue, we attempted to discuss the validity of our scenario and findings by benchmarking those that also performed classification tasks in patients with PD. By incorporating the same SVM-basis feature engineering and classification pipeline to learn informative EEG spectral signatures, our results showed that the PD−HC task retuned a worse accuracy (53.3%) compared with the ICD−PD counterpart (66.3%). Two aspects can explain these findings and support their validity. First, the engaged Go/NoGo task in this study induced cognitive and motor inhibition and concurrent EEG changes. The typical PD group without ICD comorbidity complications (QUIP-RS score: 0.5 ± 1.1) presumably behaved similarly to the HC group in terms of the inhibition control capability. This explained the around-chance accuracy of our PD−HC task and a noticeably large gap compared to previous PD studies [1], [2], [4], [10], [14], [16] that distinguished PD from HC subjects using task-free resting EEG data (sample-wise and subject-wise validation accuracy: 81−99%; Table I). Second, the ICD group (i.e., QUIP-RS score: 16.0 ± 12.3) did conform to the preferable Go/NoGo rationale. Thus, the SVM pipeline was allowed to learn the underlying EEG distinction in the ICD−PD task, leading to an above-chance accuracy of 66.3%. The studies listed in Table I suggest that it is more challenging to differentiate between motor or non-motor subtypes in patients with PD than to solely diagnose subjects as having PD or not; classifying, for example, early or late stage for 86.4% [18], presence of cognitive worsening for 82% [23], FOG or normal walking for 80.2% [20], and presence of MCI for 66% [21]. Furthermore, [21] not only tackled a cognitive comorbidity in patients with PD but also conceived a similar methodological framework in terms of EEG spectral features, SVM modeling, and realistic subject-wise CV, which could be regarded a direct support to our ICD−PD classification outcome.

By contrast, this study implemented an SVR pipeline to estimate the ICD severity of individuals with PD by learning the links between EEG spectral disparity and the clinical QUIP-RS score. Given the lack of relevant reports, this study verified the effectiveness by comparison with random guessing. The ICD group corresponded to higher SVR-estimated scores than the PD group. This tendency significantly resembled the ICD−PD gap in the clinical questionnaire score, which was barely replicated by random estimation (Table III). Nevertheless, as indicated by the individual outcomes, the implemented SVR modeling likely underestimated the patients with severe ICD comorbidity or misestimated typical patients to have mild ICD comorbidity (i.e., overestimated scores). This outcome could be mainly attributed to the small sample size of the ICD group (9 subjects) versus the PD group (21 subjects) recruited in this study. Most critically, the annotated QUIP-RS data manifested dominantly in minor scores (patients with typical PD without ICD) but sparsely from mild to severe scores (patients with PD and ICD) within the range of 0–64. Thus, the diversity-limited score spectrum could introduce challenges in learning a highly skewed ICD score distribution using SVR. The sparseness of ICD subjects may also explain, in part, the suboptimal performance in distinguishing them from typical PD subjects (sensitivity: 61.1%; specificity: 68.6%) in the ICD−PD classification task (Table II).

In short, despite follow-up efforts required to enhance the performance, both the demonstrated SVM-basis ICD−PD classification and SVR-basis ICD severity estimation were encouraging and explainable. We believe that this study is valid for proving the applicability of objectively assessing ICD comorbidities in PD during pharmacological intervention using an EEG-driven machine-learning scenario.

C. Future Work

The encouraging results warrant future efforts to develop an accurate BCI-based ICD comorbidity detection infrastructure and deploy it as a neurological evidence-based CAD system to assist traditional diagnostic approaches. First, enlarging the patient sample size is one of the dominant factors in improving machine-learning efficacy, particularly for those with severe ICD comorbidities. In addition, a longitudinal study of the same individual with PD during their chronic DA intervention is required to appraise the generalizability of a pre-trained predictive model over time, given the realistic intra-individual EEG variability [42], [43]. Second, recent BCI studies have reported the success of advanced spectral feature mining [44], deep learning [45], and transfer learning [46], facilitating the modeling of EEG activity in response to tasks of interest. These methodological advantages could potentially augment ICD modeling in individuals with PD. Finally, follow-up reinforcement for the hardware aspect may reinvent a LEGO headset-mounted miniature amplifier and incorporate a display goggle. An all-in-one, standalone EEG headset is an easy-to-access, user-friendly wearable CAD device for objective screening, prognostic monitoring, and early detection of cognitive comorbidities in clinical practice or at home.

V. Conclusion

This study proposed an EEG-driven machine-learning scenario to assess ICD symptoms in patients with PD when attentively engaging in a cognitive Go/NoGo task. Moreover, EEG measurements were performed using a low-cost custom device rather than a commercial high-precision product. The results showed that our scenario enabled the effective identification of patients with PD and ICD comorbidities and estimated the ICD comorbidity severity, which was barely replicated by analytical benchmarks without actual ICD information. Such a demonstration facilitates the deployment of a wearable BCI-based CAD system to routinely monitor the adverse cognitive effects of ICD comorbidities in patients with PD during chronic DA intervention for motor symptoms.

References

[1] R. Yuvaraj, U. R. Acharya, and Y. Hagiwara, "A novel Parkinson's disease diagnosis index using higher-order spectra features in EEG signals," *Neural Comput. Appl.*, vol. 30, no. 4, pp. 1225–1235, Aug. 2018.

[2] S. L. Oh et al., "A deep learning approach for Parkinson's disease diagnosis from EEG signals," *Neural Comput. Appl.*, vol. 32, pp. 10927–10933, Aug. 2018.

[3] R. G. Brown and C. D. Marsden, "Cognitive function in Parkinson's disease: From description to theory," *Trends Neurosci.*, vol. 13, no. 1, pp. 21–29, Jan. 1990.

[4] S. Lee, R. Hussein, R. Ward, Z. J. Wang, and M. J. McKeown, "A convolutional-recurrent neural network approach to resting-state EEG classification in Parkinson's disease," *J. Neurosci. Methods*, vol. 361, Sep. 2021, Art. no. 109282.

[5] G. M. Meyer et al., "Inhibitory control dysfunction in parkinsonian impulse control disorders," *Brain*, vol. 143, no. 12, pp. 3734–3747, Dec. 2020.

[6] D. Weintraub et al., "Impulse control disorders in Parkinson disease: A cross-sectional study of 3090 patients," *Arch. Neurol.*, vol. 67, no. 5, pp. 589–595, May 2010.

[7] T. C. Napier et al., "Linking neuroscience with modern concepts of impulse control disorders in Parkinson's disease," *Movement Disorders*, vol. 30, no. 2, pp. 141–149, Feb. 2015.

[8] C. Spay et al., "Resting state oscillations suggest a motor component of Parkinson's impulse control disorders," *Clin. Neurophysiol.*, vol. 130, no. 11, pp. 2065–2075, Nov. 2019.

[9] G. M. Meyer, C. Spay, C. Laurencin, B. Ballanger, G. Sescousse, and P. Boulinguez, "Functional imaging studies of impulse control disorders in Parkinson's disease need a stronger neurocognitive footing," *Neurosci. Biobehav. Rev.*, vol. 98, pp. 164–176, Mar. 2019.

[10] C. Chu et al., "Deep learning reveals personalized spatial spectral abnormalities of high delta and low alpha bands in EEG of patients with early Parkinson's disease," *J. Neural Eng.*, vol. 18, no. 6, Dec. 2021, Art. no. 066036.

[11] M. Pondal et al., "Clinical features of dopamine agonist withdrawal syndrome in a movement disorders clinic," *J. Neurol. Neurosurg. Psychiatry*, vol. 84, no. 2, pp. 130–135, Feb. 2013.

[12] V. Voon et al., "Dopamine agonists and risk: Impulse control disorders in Parkinson's disease," *Brain, J. Neurol.*, vol. 134, no. 5, pp. 1438–1446, 2011.

[13] Y. P. Lin et al., "Objective assessment of impulse control disorder in patients with Parkinson's disease using a low-cost LEGO-like EEG headset: A feasibility study," *J. Neuroeng. Rehabil.*, vol. 18, no. 1, p. 109, Jul. 2021.

[14] K.-H. Chang et al., "Evaluating the different stages of Parkinson's disease using electroencephalography with Holo–Hilbert spectral analysis," *Frontiers Aging Neurosci.*, vol. 14, May 2022, Art. no. 832637.

[15] C. M. McCrimmon et al., "Performance assessment of a custom, portable, and low-cost brain–computer interface platform," *IEEE Trans. Biomed. Eng.*, vol. 64, no. 10, pp. 2313–2320, Oct. 2017.

[16] S. A. Khoshnevis and R. Sankar, "Diagnosis of Parkinson's disease using higher order statistical analysis of alpha and beta rhythms," *Biomed. Signal Process. Control*, vol. 77, Aug. 2022, Art. no. 103743.

[17] P. G. Vinoj, S. Jacob, V. G. Menon, S. Rajesh, and M. R. Khosravi, "Brain-controlled adaptive lower limb exoskeleton for rehabilitation of post-stroke paralyzed," *IEEE Access*, vol. 7, pp. 132628–132648, 2019.

[18] S. A. Khoshnevis and R. Sankar, "Classification of the stages of Parkinson's disease using novel higher-order statistical features of EEG signals," *Neural Comput. Appl.*, vol. 33, no. 13, pp. 7615–7627, Jul. 2021.

[19] M. Nakanishi et al., "Detecting glaucoma with a portable brain-computer interface for objective assessment of visual function loss," *JAMA Ophthalmol.*, vol. 135, no. 6, pp. 550–557, Jun. 2017.

[20] A. M. A. Handojoseno et al., "Analysis and prediction of the freezing of gait using EEG brain dynamics," *IEEE Trans. Neural Syst. Rehabil. Eng.*, vol. 23, no. 5, pp. 887–896, Sep. 2015.

[21] J. Zhang et al., "Identifying Parkinson's disease with mild cognitive impairment by using combined MR imaging and electroencephalogram," *Eur. Radiol.*, vol. 31, no. 10, pp. 7386–7394, Oct. 2021.

[22] N. Betrouni et al., "Electroencephalography-based machine learning for cognitive profiling in Parkinson's disease: Preliminary results," *Movement Disorders*, vol. 34, no. 2, pp. 210–217, Feb. 2019.

[23] D. Arnaldi et al., "Prediction of cognitive worsening in de novo Parkinson's disease: Clinical use of biomarkers," *Movement Disorders*, vol. 32, no. 12, pp. 1738–1747, Dec. 2017.

[24] J. Mei, C. Desrosiers, and J. Frasnelli, "Machine learning for the diagnosis of Parkinson's disease: A review of literature," *Frontiers Aging Neurosci.*, vol. 13, pp. 1–12, May 2021.

[25] M. Xu, F. He, T.-P. Jung, X. Gu, and D. Ming, "Current challenges for the practical application of electroencephalography-based brain–computer interfaces," *Engineering*, vol. 7, no. 12, pp. 1710–1712, Dec. 2021.

[26] K.-C. Chuang and Y.-P. Lin, "Cost-efficient, portable, and custom multi-subject electroencephalogram recording system," *IEEE Access*, vol. 7, pp. 56760–56769, 2019.

[27] Y.-P. Lin, T.-Y. Chen, and W.-J. Chen, "Cost-efficient and custom electrode-holder assembly infrastructure for EEG recordings," *Sensors*, vol. 19, no. 19, p. 4273, Oct. 2019.

[28] W.-J. Chen and Y.-P. Lin, "Event-related potential-based collaborative brain–computer interface for augmenting human performance using a low-cost, custom electroencephalogram hyperscanning infrastructure," *IEEE Trans. Cognit. Develop. Syst.*, early access, Feb. 15, 2023, doi: 10.1109/TCDS.2023.3245048.

[29] S.-Y. Yang and Y.-P. Lin, "Validating a LEGO-like EEG headset for a simultaneous recording of wet- and dry-electrode systems during treadmill walking," in *Proc. 42nd Annu. Int. Conf. IEEE Eng. Med. Biol. Soc. (EMBC)*, Jul. 2020, pp. 4055–4058.

[30] J. R. Wessel, "Prepotent motor activity and inhibitory control demands in different variants of the go/no-go paradigm," *Psychophysiology*, vol. 55, no. 3, Mar. 2018, Art. no. e12871.

[31] F. Zamorano et al., "Temporal constraints of behavioral inhibition: Relevance of inter-stimulus interval in a Go-Nogo task," *PLoS ONE*, vol. 9, no. 1, Jan. 2014, Art. no. e87232.

[32] S. Baumeister et al., "Sequential inhibitory control processes assessed through simultaneous EEG–fMRI," *NeuroImage*, vol. 94, pp. 349–359, Jul. 2014.

[33] A. J. Hughes, Y. Ben-Shlomo, S. E. Daniel, and A. J. Lees, "What features improve the accuracy of clinical diagnosis in Parkinson's disease: A clinicopathologic study," *Neurology*, vol. 42, no. 6, pp. 1142–1146, Jun. 1992.

[34] D. Weintraub, E. Mamikonyan, K. Papay, J. A. Shea, S. X. Xie, and A. Siderowf, "Questionnaire for impulsive-compulsive disorders in Parkinson's disease-rating scale," *Movement Disorders*, vol. 27, no. 2, pp. 242–247, Feb. 2012.

[35] T. P. Jung et al., "Removing electroencephalographic artifacts by blind source separation," *Psychophysiology*, vol. 37, no. 2, pp. 78–163, Mar. 2000.

[36] A. Delorme and S. Makeig, "EEGLAB: An open source toolbox for analysis of single-trial EEG dynamics including independent component analysis," *J. Neurosci. Methods*, vol. 134, no. 1, pp. 21–29, Mar. 2004.

[37] S. Makeig, "Auditory event-related dynamics of the EEG spectrum and effects of exposure to tones," *Electroencephalogr. Clin. Neurophysiol.*, vol. 86, no. 4, pp. 283–293, Apr. 1993.

[38] C.-C. Chang and C.-J. Lin, "LIBSVM: A library for support vector machines," *ACM Trans. Intell. Syst. Technol.*, vol. 2, no. 3, pp. 1–27, Apr. 2011.

[39] H. Peng, F. Long, and C. Ding, "Feature selection based on mutual information criteria of max-dependency, max-relevance, and min-redundancy," *IEEE Trans. Pattern Anal. Mach. Intell.*, vol. 27, no. 8, pp. 1226–1238, Aug. 2005.

[40] J. N. Caviness et al., "Both early and late cognitive dysfunction affects the electroencephalogram in Parkinson's disease," *Parkinsonism Related Disorders*, vol. 13, no. 6, pp. 348–354, Aug. 2007.

[41] M. Cai et al., "Identifying mild cognitive impairment in Parkinson's disease with electroencephalogram functional connectivity," *Frontiers Aging Neurosci.*, vol. 13, pp. 1–12, Jul. 2021.

[42] Y.-P. Lin, "Constructing a personalized cross-day EEG-based emotion-classification model using transfer learning," *IEEE J. Biomed. Health Informat.*, vol. 24, no. 5, pp. 1255–1264, May 2020.

[43] Y.-W. Shen and Y.-P. Lin, "Challenge for affective brain–computer interfaces: Non-stationary spatio-spectral EEG oscillations of emotional responses," *Frontiers Hum. Neurosci.*, vol. 13, p. 366, Oct. 2019.

[44] Y. Pei et al., "A tensor-based frequency features combination method for brain–computer interfaces," *IEEE Trans. Neural Syst. Rehabil. Eng.*, vol. 30, pp. 465–475, 2022.

[45] E. Santamaría-Vázquez, V. Martínez-Cagigal, F. Vaquerizo-Villar, and R. Hornero, "EEG-inception: A novel deep convolutional neural network for assistive ERP-based brain–computer interfaces," *IEEE Trans. Neural Syst. Rehabil. Eng.*, vol. 28, no. 12, pp. 2773–2782, Dec. 2020.

[46] H. He and D. Wu, "Transfer learning for brain–computer interfaces: A Euclidean space data alignment approach," *IEEE Trans. Biomed. Eng.*, vol. 67, no. 2, pp. 399–410, Feb. 2020.